Active Power Filter for Power Quality Enhancement of Photovoltaic Renewable Energy Systems

Mohamed Amin Moftah[1], *Egyptian Electricity Transmission Company, Egypt*, Gaber El-Saady[2] and El-Noby A. Ibrahim[2], *Electrical Engineering Department, Faculty of Engineering, Asyut University , Egypt*

Abstract-- **This paper introduces an application of active power filter (APF) in photovoltaic (PV) renewable energy system for power quality (PQ) improvement. The PV energy system is connected to Saudi Arabia National Grid (110/13.8/0.4 KV) via inverter circuit, transmission line and step-up transformer. The harmonics due to the inverter circuit and non-linear local load are mitigated and reduced using shunt APF. Also the reactive power and then the voltage regulation can be adapted and adjusted using APF. Design of APF is presented. The system under study is simulated using MATLAB/SIMULINK Software Package. The APF structure and its control system is also presented. The simulated system is subjected to loading disturbances to study the effectiveness of APF. The digital results prove the powerful of the APF in sensing of deceasing the total harmonic distortion (THD) and fast voltage regulation.**

Index Terms-- **distributed generation, photovoltaic system, active power filter, harmonics mitigation, power factor correction, hysteresis band current controller and power quality.**

I. Introduction

Connection of the traditional electrical utility networks with renewable energy sources like PV, wind, diesel engine, fuel cell etc., has bring a series of new challenges to PQ. The major research topic in the power distribution system is to improve the PQ [1]-[2]. The primary cause for poor PQ is the arrival of power electronics based devices and non-linear loads in both industrial/commercial sector and domestic environment [3]. Effects of poor PQ like sag, swell distortion in waveform, harmonics, reactive power generation has affected both grid as well as utility sectors. Therefore, efficient solutions for solving these pollution problems have become highly critical.

Active and passive filters are used for mitigation, elimination or reduction of these effects. Passive power filters (PPF) have many disadvantages [4], such as their inability to compensate random harmonic current variation; they are designed only for a specific frequency and the possibility of resonance at point of common coupling (PCC), tuning problems and filter overloading. The other drawback of PPFs is that the sizes of required elements are bulky elements.

There are many research efforts to improve the efficiency of the PV system. They aimed at the supplying grid with active and reactive power, to reduce the harmonics in the system, [5]-[11]. The PV system supply real power from PV arrays to load and support reactive and harmonics power simultaneously.

Nowadays APFs have become the most effective solution to eliminate harmonic pollution in power systems and have attracted much attention because of their advantages; (i) Capability to compensate random varying currents. (ii) Good controllability and fast response to system variations. (iii) High control accuracy. So APFs appear to be a viable solution for controlling harmonics-associated problems.

In operation, the APF injects compensation currents at PCC into the AC lines equal but opposite direction distortion as well as absorbing or generating reactive power, thereby eliminate the unwanted harmonics and compensate for reactive power of the connected load [12]. In this way, the APF cancels out the harmonic currents and leaves the fundamental current component to be provided by the power system and improve the system power factor [13], Furthermore shunt APF can keep the power system balanced under the condition of the unbalanced and the nonlinear loads. By this methodology harmonic suppression is possible within permissible standards as defined by IEEE-519.

The application of APFs for mitigating harmonic currents and compensating for reactive power of PV renewable energy source feeding nonlinear load was presented in this paper.

II. Nonlinear Loads and Harmonic Distortion

Nonlinear loads are mainly electronic equipment which has a rectification stage like: computers, electronic ballasts, motor drives, and light emitting diode lights, etc. Harmonic distortion can shorten the life of the appliances by voltage stress and increased heating of electrical insulation. The effect of harmonics in distribution system lines increases losses and generally degrades the quality of the supply.

[1]Mohamed Amin Moftah is at HV S/S Projects Section, Middle Egypt Electricity Zone, Egyptian Electricity Transmission Company, Egypt (mhmoftah6666@yahoo.com) Tel: +201006803030.

[2]Gaber El-Saady & El-Noby A. Ibrahim, mail: (El-Saady@aun.edu.eg).

III. PV SYSTEM TOPOLOGY

The basic power scheme of the studied system is shown in Fig. 1. A PV system is connected to a three phase utility grid (Saudi Arabia National Grid, 110/13.8/0.4 KV) with shunt APF interface and non-linear load. The PV system used to generate power from the sun array and feeding to both grid and local nonlinear load. The shunt APF used to enhance PQ of the photovoltaic generation and hence the infinite bus grid. So two current controlled voltage source inverters (VSI) namely; PV inverter and APF inverter are connected to each other in the system. The PV inverter used to convert DC power to AC power and to properly ensure a power sharing of the load demand under various irradiance levels between the PV array and the grid. The APF inverter used to compensate both the reactive power and harmonics, caused by the nonlinear load at PCC of the AC mains. Hence APF inverter reduce low-frequency ripple problem in the system, [14].

PV and APF inverters output power will follow the power references. The instantaneous reactive power (IRP) p–q theory is used for generating reference signals for control of power inverters [15]-[19]. The calculation of active and reactive components of modulating currents follows the method of instantaneous power theory [15]. Hysteresis pulse width modulation technique has been applied in the control algorithm of both PV and APF inverters.

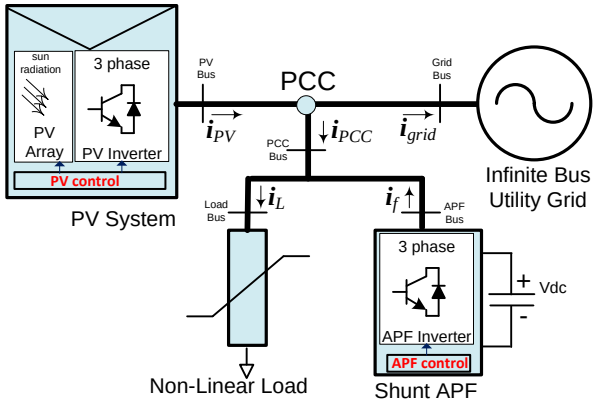

Fig. 1. PV System with APF basic schematic diagram.

A. PV Module

A photovoltaic system converts sunlight into electricity. The basic device of a photovoltaic system is the PV cell [20]. PV cells produce less than 3W at 0.5 to 0.6 Volts, so cells are connected in series to produce enough power and grouped to form PV modules or panels. Panels can be grouped to form large photovoltaic arrays. The term array is usually employed to describe a photovoltaic panel (with several cells connected in series and/or parallel) or a group of panels. There are different sizes of PV module commercially available.

The ideal solar cell can, theoretically, be modeled as a current source in anti-parallel with a diode. The equivalent circuit of a single diode PV cell [21] is depicted in Fig. 2. In the ideal PV cell, series resistance (R_s =0, no series loss) and shunt resistance (R_{sh} = infinite, no leakage to ground). The PV cell terminal current (I_{pv}) is equal to the light produced current (I_{ph}), less the diode current (I_d) *and* the shunt leakage current (or ground-shunt current, I_{sh}). The series resistance (R_s) represents the internal resistance to the current flow. The shunt resistance (R_{sh}) is inversely related to leakage current to the ground.

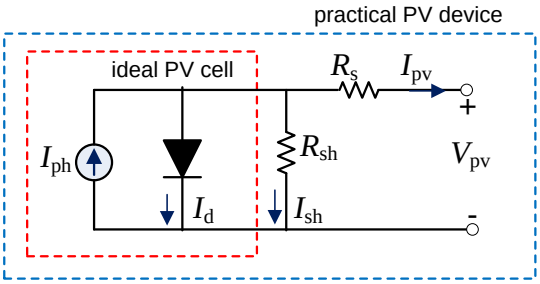

Fig. 2. The electrical equivalent circuit model of PV cell

Applying Kirchhoff's law [22] on the equivalent circuit in Fig. 2. , the current produced by the solar cell can be formulated as:

$$I_{pv}=I_{ph}-I_{\circ}\left[\exp\left(\frac{\left(V_{pv}+I_{pv}R_S\right)}{\alpha KT/q}-1\right)\right]-\left(\frac{V_{pv}+I_{pv}R_S}{R_{sh}}\right) \quad (1)$$

Where, I_{ph} is photo-current generated by the solar irradiation to the p-n junction cell; I_o is diode saturation current; q is Coulomb constant (1.602×10^{-19} C); K *is* Boltzmann's constant (1.381×10^{-23} J/K); T is cell temperature in ^oK; α is p-n junction ideality factor of the diode (1 for an ideal diode); R_s and R_{sh} are series and shunt resistances of the PV cell, respectively.

For PV array consisting of N_s series and N_p parallel connected PV modules, (1) becomes:

$$I_{pv}=N_p\left\{I_{ph}-I_{\circ}\left[\exp\left(\frac{\left(V_{pv}+I_{pv}R_S\right)}{N_SV_T}-1\right)\right]-\left(\frac{V_{pv}+I_{pv}R_S}{R_{sh}}\right)\right\} \quad (2)$$

As the value of R_{sh} is very large, it has a negligible effect on the I-V characteristics of PV cell or array. Thus (2) can be simplified to:

$$I_{pv}=N_p\left\{I_{ph}-I_{\circ}\left[\exp\left(\frac{\left(V_{pv}+I_{pv}R_S\right)}{N_SV_T}-1\right)\right]\right\} \quad (3)$$

Where, V_T is the thermal voltage of the array with N_s cells connected in series, (V_T= α.K.T/q). Cells connected in parallel increase the PV current and cells connected in series provide greater PV output voltages.

B. The Scheme of 3-Phase PV Grid-Connected Inverter

In grid connected inverter, the inverter is operated as a voltage source or a current source. When the inverter is operated as a voltage source, the grid-connection system can be equivalent to parallel connection of two voltage sources. In this mode, the output current injected into grid depends on the grid voltage quality. If the grid voltage is distorted, the exported output current is distorted. Therefore this scheme is

not a good choice for grid-connection system [23]. Current controlled mode has been chosen for this work to operate the inverter as a current source, because this minimizes the effect of voltage harmonics on the output current and improves PQ.

Fig. 3. illustrates, the electrical diagram of power and control stages of PV VSI connected to a grid (110/13.8/.4KV, 60Hz as an infinite bus network). The power loop is on top of the control loop in order to explain the key of how to control output current of the PV inverter. This is in addition to the control of PV active and reactive powers.

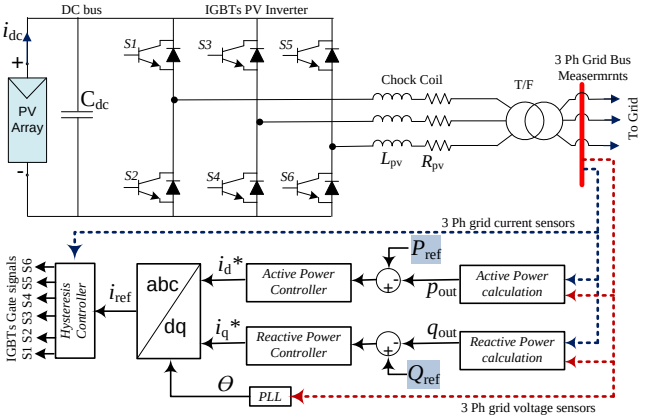

Fig. 3. Electrical diagram for PV inverter

The PV inverter is fed from a PV panel and connected to the grid through inductor (L_{pv}). The main target of the PV inverter is to inject current from the PV panel at a power factor within a certain range. The system in Fig. 3 composed of a PV panel, input capacitor (C_{dc}), three arms full bridge inverter, each arm has two ideal semiconductor switches (IGBTs) with a reverse diode in anti-parallel, coupling inductor (L_{pv}, R_{pv}.), output current/voltage sensors and DC bus voltage sensor.

Output voltage and frequency of PV VSI should be same as that of grid voltage and frequency. So the grid synchronizing angle (Θ) obtained from phase locked loop (PLL) control is implemented to generate unity vector template.

C. Control of PV Grid-Connected Inverter

Power flow to and from the utility grid can only be controlled through a current mode control scheme, because the voltage is always dictated to the inverter by the grid. In this paper, pulse width modulation voltage source inverter (PWM-VSI) of the PV system uses a hysteresis current control, also known as adaptive current control.

With this control, the PV VSI upper and lower IGBT switches are turned on and off in such a way as to keep the PV output currents tracking their references with a very small amplitude error or phase delay. Using a bipolar switching scheme, the PV VSI current can be controlled to the grid by presenting either a positive or negative polarity of the PV DC bus voltage to one side of the VSI side inductor. According to the result $di/dt = V/L$, the polarity of the voltage across the inductor determines the direction of change in current magnitude. The PV VSI at any instant can change this polarity because the PV DC bus voltage always higher in magnitude than the voltage presented by the grid. Thus, the PV inverter can also dictate the direction of current change at any instant. It is desired that the current through the PV interface inductor (to and from the grid) stay as close to the defined set point as possible. Tolerance band control uses this fundamental behavior of current through inductors to make the actual current 'dance' around the desired set point as illustrated in next subsections.

This control scheme for PV is suitable for the injection of both active and reactive power into a grid. It enables PV inverter to absorb little active power from grid, regulate PV VSI DC bus voltage within limits, and inject the required reactive power. The positive effect of reactive power support has been highlighted showing benefits on grid current and voltage profiles. To improve the PQ of the electric power system and to compensate the reactive power of the load, the capacitive reactive power for power factor correction is supplied by PV system.

D. Calculation of PV VSI Reference Currents

As shown in Fig. 4. , the PV VSI reference currents are generated by the sine generator based on the voltage phase and the given amplitude of output current. The reference current (i_{ref}) subtracts the grid current (i_g) creating error current (i_e) which goes through three-level hysteresis controller to obtain signals for switching PV full-bridge VSI.

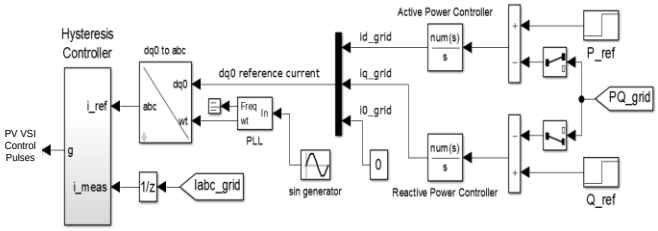

Fig. 4. Generation of PV inverter control pulses

For a given complex power set-point $S_{ref} = P_{ref} + j\,Q_{ref}$ and an output voltage of $v_o = v_{od} + j\,v_{oq}$, Thus, the reference current signals i^*_d and i^*_q can be calculated with:

$$\begin{bmatrix} i_d^* \\ i_q^* \end{bmatrix} = \frac{1}{v_{od}^{\,2} + v_{oq}^{\,2}} \begin{bmatrix} v_{od} & v_{oq} \\ v_{oq} & -v_{od} \end{bmatrix} \cdot \begin{bmatrix} P_{ref} \\ Q_{ref} \end{bmatrix} \qquad (4)$$

Where P_{ref} and Q_{ref} are reference active and reactive power signals. Reference current signals in three-phase system are calculated by reverse Clark transformation (*qd0 to abc*). In order to achieve high output current quality, a low-pass filtering of the signal generated from subtracting the grid-side current I_g from the reference current I_{ref} as shown in Fig. 5.

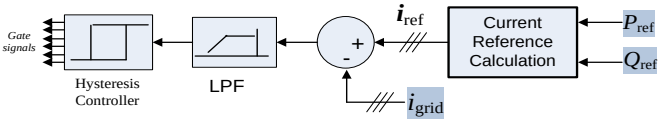

Fig. 5. PV Power Controller Block Diagram

In the case of grid-feeding PV inverter, the reference currents [i_d^*, i_q^*] are usually provided by a power controller

[17] that regulates the active and reactive power delivered to the load as well as the grid. The instantaneous active and reactive power components are calculated by:

$$p = v_d i_d + v_q i_q \qquad q = v_d i_q - v_q i_d \tag{5}$$

The PV system control strategy is proposed for generating the inverter reference current i^*_q to inject reactive power $q = Q_{ref}$ into the grid. An appropriate control scheme can help the inverter operate in reactive power compensation mode even with the absence of active input power. Operating PV inverter in VAR mode involves two steps (i) Pre-charging the PV DC bus capacitance $C_{dc.}$ (ii) Regulating the PV DC bus voltage within limits while regulating the injected reactive power.

In order to overcome PV inverter losses while supplying the required power, the inverter needs to draw some active power from the grid. The control strategy enables PV inverters to absorb little active power from the grid when the PV source (e.g. sun) is not available to compensate for the inverters" internal losses, regulates the DC bus voltage to keep it within limits, and operates the inverters in VAR mode. This eventually extends the utilization of PV inverters beyond active power generation and helps improving grid stability and voltage regulation [24]-[25]. For unity power factor, $Q_{ref} = 0$ and the reference grid current will be:

$$i_d^* = \frac{v_{od}}{v_{od}^2 + v_{oq}^2}.P_{ref} \quad , \quad i_q^* = \frac{v_{oq}}{v_{od}^2 + v_{oq}^2}.P_{ref} \tag{6}$$

Active and reactive power control can be achieved by controlling direct and quadrature current components (*dq*), respectively. Two control loops are used to control PV active and reactive power, respectively as depicted in Fig. 3. Active power reference is used to set the d-axis current reference for active power control. This assures that all the power coming from the PV is instantaneously transferred to the load as well as the grid by the PV inverter.

IV. THE PROPOSED SHUNT APF CONFIGURATION

A. Shunt APF System Structure and Work Principle

The structure of shunt APF system is shown in Fig.6 and can be divided into *four parts*: optimal reference current extractor, compensation current control, gate driver and main current controlled voltage source inverter (CC-VSI) power circuit. Each component of the proposed APF system will be explained in the following subsections.

The main feature of the APF (which sometimes called active harmonic filter or line conditioner) is that, the supply current (i_{pcc}) is forced to be sinusoidal and in phase with the supply voltage (v_{pcc}) regardless of the characteristics of the load, (i.e. shunt APF acts as a parallel current source with the nonlinear load) using the relation:

$$i_{pcc} = i_L - i_f \tag{7}$$

Where (i_f) is the filter compensation current. Suppose the nonlinear load current (i_L) can be written as the sum of the fundamental current component ($i_{L,f}$) and the current harmonics ($i_{L,h}$) according to the following equation:

$$i_L = i_{L,f} + i_{L,h} \tag{8}$$

Then the injected filter compensation current (i_f) by the shunt APF should be:

$$i_f = i_{L,h} \tag{9}$$

The resulting current at PCC as source current is

$$i_{pcc} = i_L - i_f = i_{L,f} \tag{10}$$

Which contains only the fundamental component of the nonlinear load current and thus free from harmonics. Therefore, the shunt APF is harmonics cancellation and reactive power compensation by injecting equal but opposite harmonics and reactive currents into the supply line.

B. The Main Circuit Description of Shunt APF.

The proposed three phase shunt APF shown in Fig.6 consists of (i) the three-leg CC-VSI power switches having six IGBTs with anti-paralleling diodes, to provide a mechanism for bi-directional flow of compensation current to be either absorbed from or injected into the supply system. (ii) DC bus (V_{dc}) connected common to 3-Leg APF VSI, serves as an energy supply for APF. (iii) APF interface reactor (L_f) connected on the AC side of the VSI at PCC to regulate the maximum allowable magnitude ripple current flow into the APF. (iv) Finally the controller, which has to be established in order to actively shape the supply current to sinusoidal wave shape of a unity power factor.

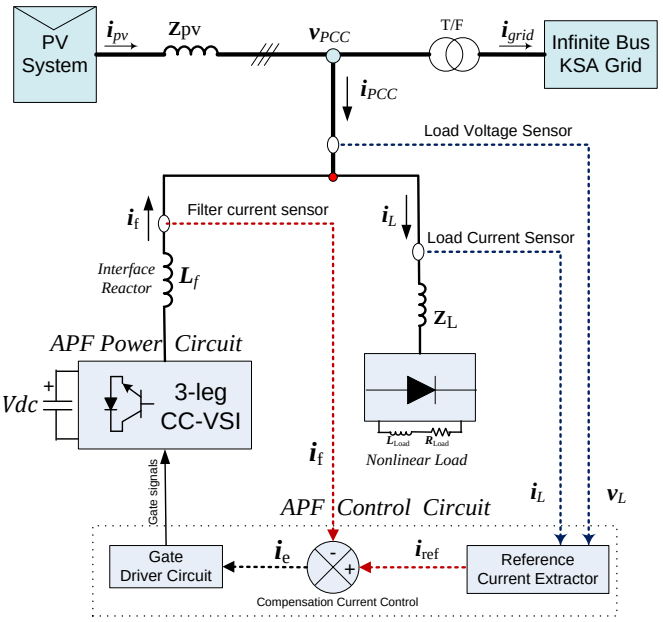

Fig. 6. Structure of shunt APF system interfaced to PV system

V. CONTROL STRATEGY OF PROPOSED SHUNT APF

A. General

The control system for shunt APF could be divided into two main stages. In the first stage the reference compensating current has to be determined, while in the second stage the derivation of the switching function for the filter inverter circuit VSI is computed.

B. APF Reference Compensation Current Calculation

The instantaneous reactive power IRP theory that is well known as p-q control algorithm [17]-[18], is used in this study. This theorem is based on α-β orthogonal transformation, which transforms three phase load voltages (v_{La}, v_{Lb}, v_{Lc}) and load currents (i_{La}, i_{Lb}, i_{Lc}) into the stationary reference frame. From these transformed quantities, the instantaneous value of the reactive fundamental component and harmonic components are calculated. This algorithm is suitable in this case study because of the balanced load voltages and nonlinear line currents. The principle of harmonic current detection method is shown in Fig.7.

In order to get the optimal compensation reference currents ($i_{ref\text{-}a}$, $i_{ref\text{-}b}$, $i_{ref\text{-}c}$), a series of calculation would be carried out as follows:

$$\begin{bmatrix} v_\alpha \\ v_\beta \end{bmatrix} = \sqrt{\frac{2}{3}} \begin{bmatrix} 1 & -1/2 & -1/2 \\ 0 & \sqrt{3}/2 & -\sqrt{3}/2 \end{bmatrix} \cdot \begin{bmatrix} v_{La} \\ v_{Lb} \\ v_{Lc} \end{bmatrix} \quad (11)$$

$$\begin{bmatrix} i_\alpha \\ i_\beta \end{bmatrix} = \sqrt{\frac{2}{3}} \begin{bmatrix} 1 & -1/2 & -1/2 \\ 0 & \sqrt{3}/2 & -\sqrt{3}/2 \end{bmatrix} \cdot \begin{bmatrix} i_{La} \\ i_{Lb} \\ i_{Lc} \end{bmatrix} \quad (12)$$

The instantaneous real power (p) and the instantaneous imaginary power (q), both include a DC component ($\bar{p}, \bar{q}$) corresponding to fundamental of the load current and an AC component ($\tilde{p}$, $\tilde{q}$), corresponding to harmonic current of the load current, can be calculated as follows:

$$\begin{bmatrix} p \\ q \end{bmatrix} = \begin{bmatrix} v_\alpha & v_\beta \\ -v_\beta & v_\alpha \end{bmatrix} \cdot \begin{bmatrix} i_\alpha \\ i_\beta \end{bmatrix} = \begin{bmatrix} \bar{p} & \tilde{p} \\ \bar{q} & \tilde{q} \end{bmatrix} \quad (13)$$

$$and \quad p = \bar{p} + \tilde{p} \quad and \quad q = \bar{q} + \tilde{q} \quad (14)$$

In the proposed APF, the AC component ($\tilde{p}$) is extracted from p using a Low pass filter (LPF) as shown in Fig.7. The compensating currents ($i_{c\alpha}$) and ($i_{c\beta}$), which can cancel the harmonic current are derived from:

$$\begin{bmatrix} i_{c\alpha} \\ i_{c\beta} \end{bmatrix} = \frac{1}{v_\alpha^{\,2} + v_\beta^{\,2}} \begin{bmatrix} v_\alpha & -v_\beta \\ v_\beta & v_\alpha \end{bmatrix} \cdot \begin{bmatrix} \tilde{p} \\ \tilde{q} \end{bmatrix} \quad (15)$$

By taking inverse Clarke transformation matrix, the APF compensating reference currents can be calculated:

$$\begin{bmatrix} i_{ref\,a} \\ i_{ref\,b} \\ i_{ref\,c} \end{bmatrix} = \sqrt{\frac{2}{3}} \begin{bmatrix} 1 & 0 \\ -1/2 & \sqrt{3}/2 \\ -1/2 & -\sqrt{3}/2 \end{bmatrix} \begin{bmatrix} i_{c\alpha} \\ i_{c\beta} \end{bmatrix} \quad (16)$$

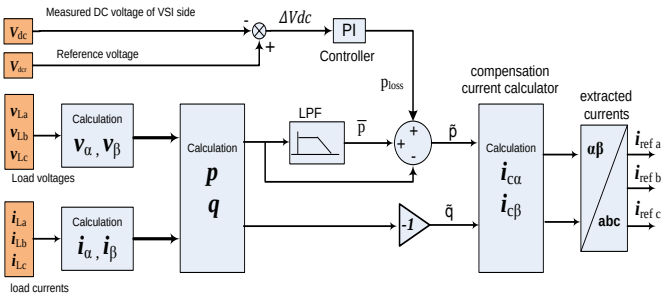

Fig. 7. p-q algorithm for the APF reference current extraction

C. Hysteresis Band Current Controller

The second stage of the shunt APF control circuit is generating appropriate gating signals for the power switches that forces the compensated filter currents (i_f) to follow derived estimated reference current (i_{ref}). The goal is to reduce the current error.

For the proposed APF in this paper, hysteresis band current control method is used because implementation of this control is simple and not expensive, the dynamic answer is excellent, and controllability of the peak-to-peak current ripple within a specified hysteresis band [27]. It allows a fast current control.

The operating principle of the hysteresis band (HB) current controller which is shown in Fig. 8, depends on comparing of measured APF VSI output current (i_f) with its reference (i_{ref}) by the hysteresis comparator. The outputs of the comparator are gating signals for the power switches.

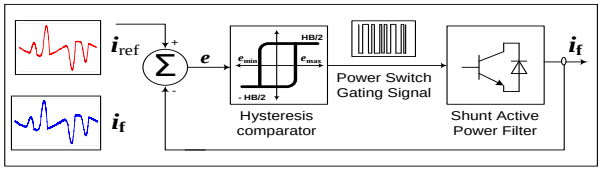

Fig. 8. Block diagram of hysteresis current controller

In this control scheme, as shown in Fig.9, a signal deviation (*HB*) is designed and imposed on (i_{ref}) to form the upper and lower limits of a hysteresis band ($i_{ref} \pm HB/2$). The filter current (i_f) is then measured and compared with (i_{ref}) ; the resulting error (e) is subjected to a hysteresis controller to determine the gating signals when exceeds the upper or lower limits set by (estimated reference signal + *HB/2*) or (estimated reference signal – *HB/2*). If the measured filter current is bigger (half of the band value) than the reference one, it is necessary to commute the corresponding power switches to decrease the output current, and it goes to the reference. *On the other hand*, if the measured current is less (half of the band value) than the reference one, the switches commute to increase output current and it goes to the reference.

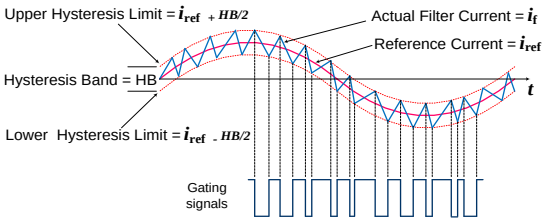

Fig. 9. Gating signal generation by hysteresis controller

As long as the error is within the hysteresis band (*HB*), no switching action is taken. Switching occurs whenever the error (e) hits the hysteresis band. The APF is therefore switched in such a way that the peak-to-peak compensation current signal (i_f) limited in a specified band around the reference current is determined by HB. The conditions of switching devices are tabulated in Table I.

TABLE I
HYSTERESIS BAND

Switch	**Hysteresis Band (HB)**
Lower switch on	$(i_{ref}\text{-}i_f) < -HB$
Upper switch on	$(i_{ref}\text{-}i_f) > HB$

VI. MODELING OF SOLAR GRID TIE SYSTEM WITH SHUNT ACTIVE POWER FILTER

To evaluate the operating performance of the designed system with and without adaptive shunt APF, a 3-phase 60Hz system is constructed using MATLAB/SIMULINK software. Fig. 10 shows the complete simulation model of PV renewable energy source tied to infinite bus Saudi Arabia Grid 110/13.8/0.4KV with APF and non-linear load for power quality improvement using hysteresis control method.

A. Modeling the Photovoltaic Array

The rated generation capacity of the PV system in this work is 50 kW, 344 V at standard Test Condition STC (1000 W/m2, 25 °C). The array configuration is achieved by connecting 10 PV modules (each 250.088 W, 34.4 V rating), in series. 20 parallel strings are combined together to design such PV array (N_s=10, N_p=20) to reach 50kW. The elemental module is TPB156x156-72-P-250W. The parameter description from the module datasheet is depicted in Table II.

TABLE II
ELECTRICAL CHARACTERISTICS DATA OF TPB156X156-72-P-250W SOLAR PANEL AT STANDARD TEST CONDITION (STC)

Parameter	Values
Maximum power (P_{max})	250.088 W
Voltage at P_{max} (V_{mpp})	34.4V
Current at P_{max} (I_{mpp})	7.27A
Open circuit voltage (V_{oc})	43.4V
Short circuit current (I_{sc})	7.89A
Temperature coefficient of I_{sc} (K_I)	(0.07±0.015 %/ºC)
Temperature coefficient of V_{oc} (K_V)	-(34±10)mV/ºC)
NOCT	(45±2) ºC)

The PV inverter uses hysteresis switching and controls active power by manipulation of direct-axis current while controlling reactive power by manipulation of quadrature-axis current. The active and reactive measurement are rated at 50kW. Therefore, an active power reference of 1pu = 50kW. The PV DC link capacitor = 1.0 mF.

B. Modeling of the remaining system parameters

The system model of 50KW PV array is connected to a 3-phase infinite bus Saudi Arabia National Grid via PV inverter through resistance and inductance (R_{pv}=*0.15 mΩ;* L_{pv} =*1.5mH*) as LC filter and step-up isolating transformer (*250KVA, 0.2/.4KV, Y/D11*).

The non-linear local load was constructed using full diode universal bridge rectifier connected in parallel with a resistor (R_{NLL}=*10* Ω) and an inductor (L_{NLL}=*90 mH*) as a load. This non-linear load tied to PV inverter output through resistance and inductance ($R_{@Load\text{-}Bus}$=*10 mΩ;* $L_{@Load\text{-}Bus}$ =*1.0 μH*). It is interfaced to the compensating shunt active power filter at 200V bus (Bus-1, Bus-2 and PCC-Bus as shown in Fig. 10.).

The proposed shunt APF connected at 200V (PCC-Bus) for compensating of both non-linear local load and PV delivered/received power to/from infinite bus 110/13.8/0.4KV Grid. The APF simulation parameters are listed in Table III.

In the three phase infinite bus grid block, the transmission line model consists of one set of RL series elements connected between input and output terminals and two sets of shunt capacitances lumped at both ends of the transmission line. Transmission line positive and zero sequence resistances, inductances and capacitances respectively are [R_1=0.1153, R_0=0.413] (Ohms/km), [L_1=1.05e^{-3}, L_0=3.32e^{-3}] (H/km) and [C_1=11.33e^{-9}, C_0=5.01e^{-9}] (F/km). Each transmission line length is depicted in Fig. 10.

TABLE III
APF AND ITS CONTROL CIRCUIT PARAMETERS

Parameter	Values
Smoothing filter	
Series Filter inductance& resistance, L_f, R_f	1.2 mH , 1μΩ
Filter DC capacitor, C_{dc}	2x40 μF
Power device (VSI)	
IGBT internal resistance, R_{on}	0.1 m Ω
Snubber resistance& capacitance, R_s, C_s	10KΩ , ∞ μF
PI Voltage regulator system	
Proportional gain for voltage regulator, K_p	0.1
Integral gain for voltage regulator, K_i	1.0
DC reference voltage, V_{dc}	850

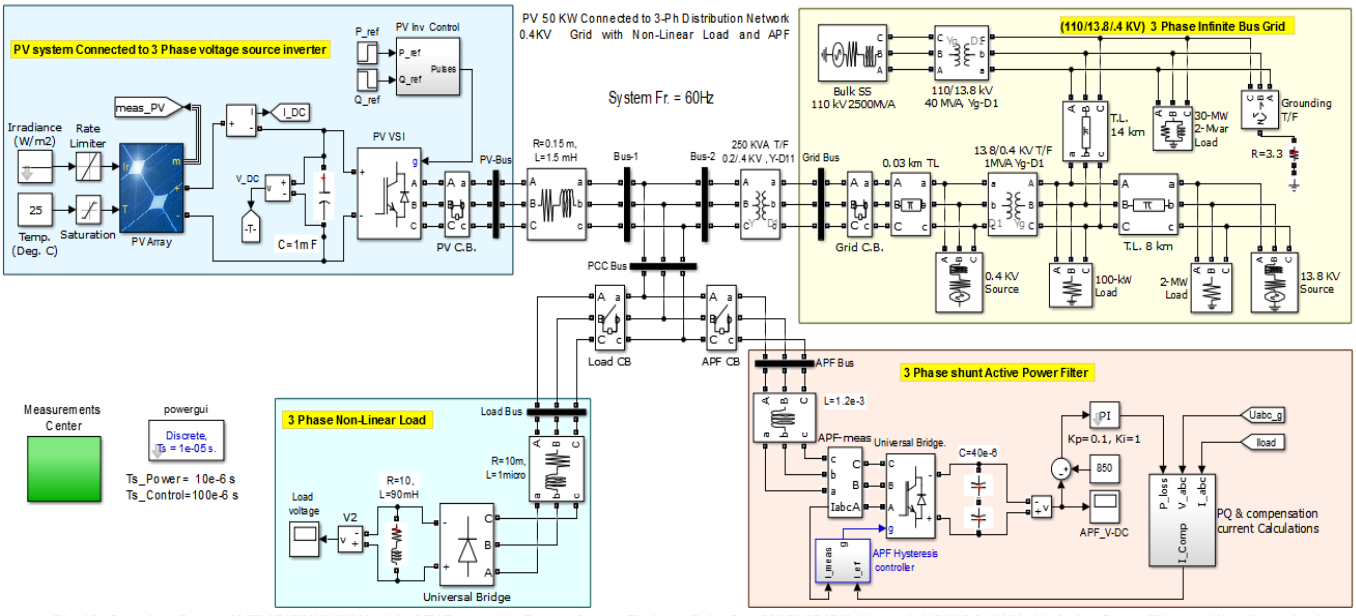

Fig. 10. Complete System MATLAB/SIMULINK Model of PV Renewable Energy Source Tied to Infinite Bus SAUDI ARABIA Network 110K/13.8/.4 KV with Active Power Filter and Non-linear load

VII. SIMULATION RESULTS AND DISCUSSION

To study the performance of the solar grid tie system in the presence of local non-linear load with the proposed shunt APF, the simulation is carried out as follows;
For the time period from t=0.0 sec till t=0.05 sec, the model is start running and both APF and non-linear load are switched OFF. So in this time period, the PV is interfaced only with utility grid. At a time t= 0.05 sec the non-linear load circuit breaker is switched ON and APF circuit breaker is still in OFF state. At a time t= 0.10 sec the non-linear load circuit breaker is still ON and APF breaker is commanded to switched ON.

The simulation measurements are conducted at different buses (PV-Bus, Bus-1, Bus-2, PCC-Bus, Grid-Bus, Load-Bus and APF-Bus), these buses are depicted in Fig. 10.

The phase "a" voltage and current waveforms and their associated THD in the three different period cases (mentioned above) are illustrated in the next simulation results figures.

Fig. 11. shows voltage waveform measured at 0.2KV PCC-Bus ($v_{PCC\text{-}a}$) , which considered the junction point between PV inverter output (Bus-1 & Bus-2) and (APF-Bus & Load-Bus). This voltage feeds the local non-linear load in the above mentioned three different cases.

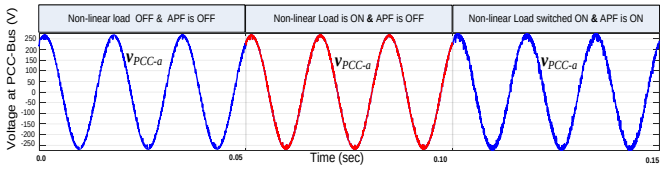

Fig. 11. Voltage waveform measured at 0.2KV PCC-Bus ($v_{PCC\text{-}a}$)

Fig. 12. shows non-linear load current measured at 0.2KV Load-Bus ($i_{L\text{-}a}$) in the above mentioned three different cases.

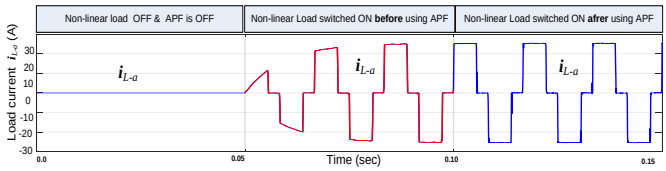

Fig. 12. Non-Linear Load current measured at 0.2KV Load-Bus ($i_{L\text{-}a}$)

Compensating filter current ($i_{f\text{-}a}$) which is to be injected at 0.2KV APF-Bus to compensate both harmonic and reactive currents caused by the non-linear load is shown in Fig. 13. This current has the ability to eliminate unwanted reactive and harmonic currents from PV output currents at 0.2KV PV-Bus and 0.4KV Grid-Bus.

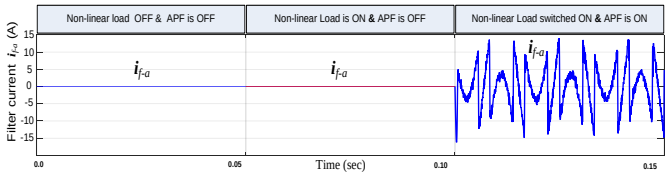

Fig. 13. Filter current injected at APF-Bus to compensate both Non-Linear load and PV currents ($i_{f\text{-}a}$)

Fig. 14. shows the current waveform at 0.2KV PCC-Bus ($i_{PCC\text{-}a}$). This current drawn from PCC for feeding the non-linear load. The FFT analysis is depicted below each case of the three different cases in the same figure.

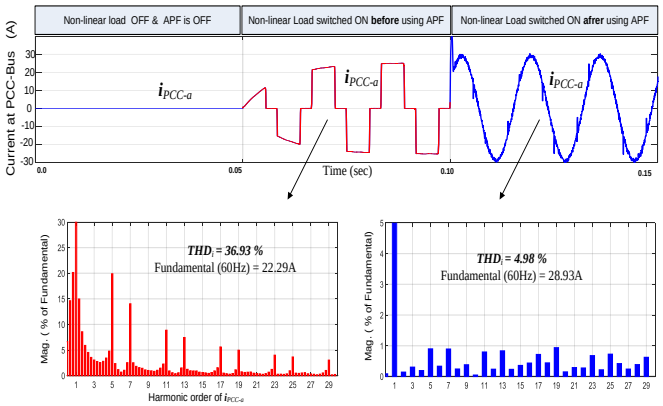

Fig. 14. Current waveform at 0.2KV PCC-Bus ($i_{PCC\text{-}a}$) and its associating FFT analysis

Through the analysis of the current waveform at 0.2KV PCC-Bus ($i_{PCC\text{-}a}$) as shown in Fig. 14, found the THD is at 36.93% before using the APF. When subjected to APF compensation at time t=0.10 sec, the waveform is now continuous, almost sinusoidal with THD about 4.98% and almost in phase with the voltage at PCC-Bus ($V_{PCC\text{-}a}$) shown in Fig. 11.

Output current delivered by PV inverter at the 0.2KV PV-Bus (i_{PV_a}) is shown in Fig. 15. This current is considered as source for supplying the non-linear load. The associating FFT analysis is depicted below each case of the three different cases in the same figure.

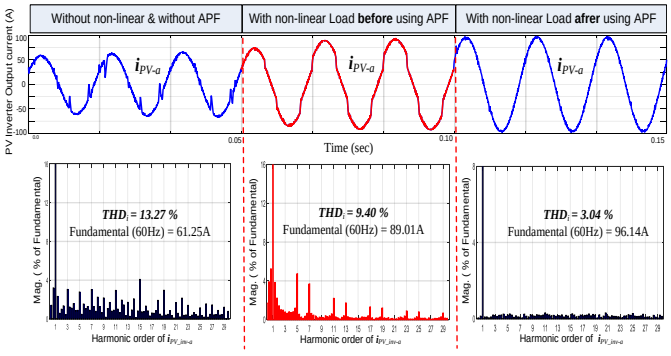

Fig. 15. Delivered output current waveform at 0.2KV PV-Bus (i_{PV_a}) and its associating FFT analysis

From Fig. 15; it is noticed that *before* connecting both the nonlinear load and the APF, the *THD* of the output current delivered by PV inverter at the PV-Bus (i_{PV_a}) is 13.27% and 9.40% respectively. While when the shunt APF is connected to the system at time t=0.10 sec, the *THD* of the output current delivered by PV inverter decreased to 3.04%; only one specter at fundamental frequency is appeared in FFT spectrum analysis, all other harmonics disappears.

Fig. 16. shows PV current submitted to the infinite bus grid (110/13.8/0.4KV Network) measured at 0.4KV Grid-Bus (i_{grid_a}). The FFT analysis is depicted below each case of the three different cases in the same figure.

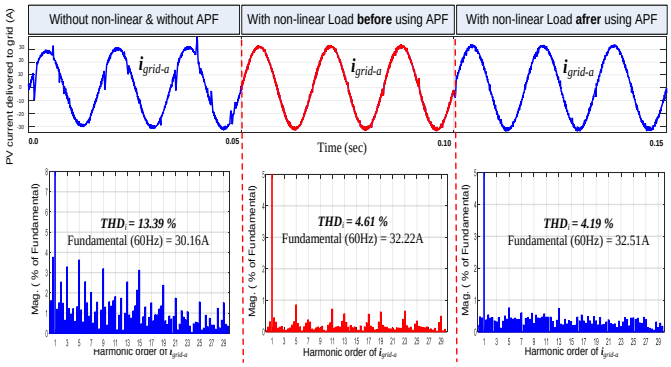

Fig. 16. Delivered output current waveform at 0.4KV Grid-Bus (i_{grid_a}) and its associating FFT analysis

Referring to Fig. 16; it is shown that *before* connecting both the nonlinear load and the APF, the *THD* of the PV current submitted to the infinite bus grid (i_{grid_a}) is 13.39% and 4.61% respectively. While after implementation of shunt active harmonic filter at time t=0.10 sec, this current waveform has become nearly sinusoidal with THD equal 4.19% as illustrated in FFT analysis in Fig. 16.

Fig. 17. shows voltage waveform measured at 0.4KV Grid-Bus ($V_{grid\text{-}a}$). From Fig. 11 & Fig.17, it was observe that voltage waveforms are always pure sinusoidal without distortion whether before connecting/disconnecting non-linear load or connecting/disconnecting the shunt active filter, which achieve excellent voltage stability.

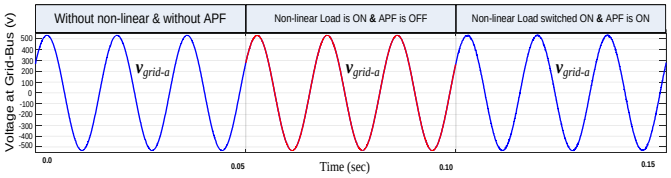

Fig. 17. Voltage waveform measured at 0.4KV Grid-Bus ($v_{grid\text{-}a}$)

Fig. 18. illustrates voltage and current waveforms ($V_{pcc\text{-}a}$ & $I_{pcc\text{-}a}$) measured at 0.2KV PCC-Bus, showing that at t=0.05 sec non-linear Load is switched ON and APF is still OFF, so the current waveform is distorted with leading phase shift about 16 degree (i.e PF ≈ 96 %). After that, at time t=0.10 sec the APF is connected. So the current waveform will be sinusoidal and exactly in phase with the voltage as shown in Fig.18. Hence the PF is near to unity, this prove the capability of APF for both reactive power and harmonics compensation and PF correction at the same time.

From the above simulation results in Fig. 11. till Fig. 18. Noting that, the values of current waveform THD decreased when the shunt APF is connected in the system compared to the values of THD without the shunt APF, as summarized in Table IV. This means that the distortions in the current waveforms are decreased and the supply current becomes almost harmonics free within acceptable standards values.

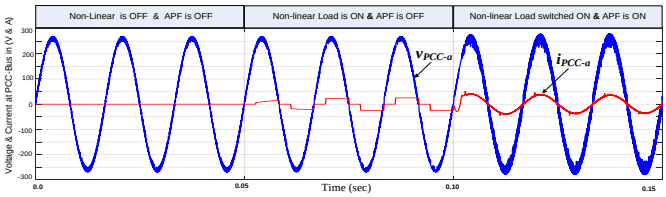

Fig. 18. Power factor measurement using voltage & current waveforms at 0.2KV PCC-Bus ($v_{pcc\text{-}a}$ / $i_{pcc\text{-}a}$)

As a final result obtained from the simulation shows that photovoltaic system connected to a three phase grid incorporating with shunt active power filter offers better sinusoidal supply waveform with approximately 77% improvement of THD reduction with almost unity power factor are achieved in the system.

TABLE IV
PV CURRENT WAVEFORMS % THD (AT PV-BUS & GRID- BUS) BEFORE AND AFTER COMPENSATION FOR PHASE "A"

Operation Scenario	% THD		
	Load=OFF APF=OFF	Load=ON APF=OFF	Load=ON APF=ON
at PV-Bus	13.27	9.40	3.04
at Grid-Bus	13.39	4.61	4.19

VIII. CONCLUSIONS

In this paper, the performance of the proposed PV renewable energy source tied to infinite bus Saudi Arabia Grid with shunt APF and non-linear load for power quality improvement using hysteresis control method was verified through simulation studies using MATLAB/Simulink under different operating conditions. This structure of shunt APF, using the instantaneous reactive power theory p-q control method, can effectively reduce the undesired effect of current harmonics from PV current and grid current.

The simulation results show that the shunt APF with adaptive control is able to adapt themselves to the load variations. As for the shunt APF, it can correct the power factor to unity besides compensating the harmonic currents present at PCC bus. The shunt APF allows the harmonics present in the utility system to be compensated, providing a good quality of PV power supply to customers through the infinite bus grid.

IX. ACKNOWLEDGMENT

The author gratefully acknowledge the management of Electrical Engineering Department, Faculty of Engineering, Asyut University for giving the opportunity and platform for the research candidate.

X. REFERENCES

[1] Khadkikar V. "Enhancing electrical power quality using UPQC": A comprehensive overview. IEEE Transaction on Power Electronics. 27(2): pp. 2284–2297; 2012.

[2] Pallagiri Venkata Dinesh Reddy, S. Chandra mouli, "Hybrid Renewable Energy Sources Based Four Leg Inverter for Power Quality Improvement", International Journal of Advanced Technology and Innovative Research, Volume.07, Issue No.06,pp.1092-1098, July-2015.

[3] Mikkili S, Panda AK. "Performance analysis and real-time implementation of shunt active filter current control strategy with type-1 and type-2 FLC triangular" M.F. International Transactions on Electrical Energy Systems. John Wiley. 24(3): pp. 347–362; 2014.
[4] Hugo. A, Ramos. C.,Aurelio. M., Gary W. C., "Real-Time Shunt Active Power Filter Compensation", IEEE TRANSACTIONS ON POWER DELIVERY, VOL. 23, NO. 4, OCTOBER 2008.
[5] S. Hyo-Ryong, et al., "Performance analysis and evaluation of a multifunctional grid-connected PV system using power hardware-in-the-loop simulation," in Applied Power Electronics Conference and Exposition (APEC), Twenty-Sixth Annual IEEE, pp. 1945-1948, 2011.
[6] F. L. Albuquerque, et al., "Photovoltaic solar system connected to the electric power grid operating as active power generator and reactive power compensator," Solar Energy, vol. 84, pp. 1310-1317, 2010.
[7] S. Dasgupta, et al., "Derivation of instantaneous current references for three phase PV inverter connected to grid with active and reactive power flow control," in Power Electronics and ECCE Asia (ICPE & ECCE), 2011 IEEE 8th International Conference on, pp. 1228-1235, 2011.
[8] Manasseh Obi, Robert Bass "Trends and challenges of grid-connected photovoltaic systems – A review", Renewable and Sustainable Energy Reviews 58, pp.1082–1094, 2016.
[9] K. Kelesidis, et al., "Investigation of a control scheme based on modified p-q theory for single phase single stage grid connected PV system," in Clean Electrical Power (ICCEP), International Conference on, pp. 535-540, 2011.
[10] R. Belaidi, et al., "Improvement of the electrical energy quality using a Shunt Active Filter supplied by a photovoltaic generator," Energy Procedia, vol. 6, pp. 522-530, 2011.
[11] C. He, et al., "A Novel Grid-Connected Converter with Active Power Filtering Function," Energy Procedia, vol. 12, pp. 348-354, 2011.
[12] G. A. Ramos, R. Costa, J. Olm, "Digital Repetitive Control under Varying Frequency Conditions" Book ,part.3,Ch.7" Shunt Active Power Filter " PP. 101-137, Springer-Verlag Berlin Heidelberg, 2013.
[13] Senthilkumar. A ,Poongothai. K, Selvakumar. S, Silambarasan. Md, P. Ajay-D-VimalRaj "Mitigation of Harmonic Distortion in Microgrid System using Adaptive Neural Learning Algorithm based Shunt Active Power Filter " SMART GRID Technologies, *Procedia Technology* 21, PP.147-154, August 2015.
[14] W. Rong-Jong and L. Chun-Yu, "Dual Active Low-Frequency Ripple Control for Clean-Energy Power-Conditioning Mechanism," *Industrial Electronics, IEEE Transactions on*, vol. 58, pp. 5172-5185, 2011.
[15] H. Akagi, S. Ogasawara, H. Kim, "The theory of instantaneous power in three-phase four-wire systems: a comprehensive approach ", IEEE Industry Applications Conference, Vol. 1 , pp.: 431-439 , 1999.
[16] F. Z. Peng, G. W. Ott, and D. J. Adams, "Harmonic and reactive power compensation based on the generalized instantaneous reactive power theory for three-phase four-wire systems," IEEE Trans. on Power Electronics, Vol. 13, No. 6, pp. 1174–1181, 1998.
[17] L. S. Czarnecki, "Instantaneous reactive power p-q theory and power properties of three-phase systems," IEEE Trans. on Power Delivery, Vol. 21, No. 1, pp. 362-367, 2006.
[18] R. S. Herrera and P. Salmerón, "Instantaneous Reactive Power Theory: A Reference in the Nonlinear Loads Compensation", IEEE Transactions on Industrial Electronics, Vol. 56, No. 6, pp. 2015-2022, June 2009.
[19] J. Rocabert, A. Luna, F. Blaabjerg, and P. Rodriguez, "Control of Power Converters in AC Microgrids", IEEE Transactions on Power Electronics, Vol. 27, No. 11, pp. 4734-4749, November 2012.
[20] Ramos Hernanz, Campayo Martín, Zamora Belver, Larrañaga Lesaka, Zulueta Guerrero, Puelles Pérez, "Modelling of Photovoltaic Module," International Conference on Renewable Energies and Power Quality (ICREPQ'10), Granada (Spain), 23th to 25th March, 2010.
[21] S. Dhar, R. Sridhar, G. Mathew, "Implementation of PV cell based standalone solar power system employing incremental conductance MPPT algorithm," in: Circuits, Power and Computing Technologies, ICCPCT, International Conference on IEEE, pp. 356–361, 2013.
[22] R. Gupta, A. Ghosh and A. Joshi, "Cascaded multilevel control of DSTATCOM using multiband hysteresis modulation", IEEE Power Eng. Soc. General Meeting, pp.18-22, Jun. 2006.
[23] K. Sayed, M. Abdel-Salam, Assiut University, Egypt "Hysteresis Current Controlled Single phase Grid-Connected PV Inverter System with LCL Filter"; Paper ID 256; Proceedings of the 15th International Middle East Power Systems Conference (MEPCON'12), Alexandria University, Egypt, December 23-25, 2012.
[24] F. Delfino, G. B. Denegri, M. Invernizzi, R. Procopio, G. Ronda, "A P-Q Capability Chart Approach to Characterize Grid Connected PV-Units ", Integration of Wide-Scale Renewable Resources Into the Power Delivery System, CIGRE/IEEE PES Joint Symposium, pp. 1-8, July 2009.
[25] Ellis, A.; Behnke, M.; Keller, J., "Simulating PV Systems in Transmission and Distribution Planning ", IEEE Power and Energy Magazine, Vol. 9, No. 3, pp. 55 – 61, 2011.
[26] Zainal Salam, Tan Perng Cheng and Awang Jusoh "Harmonics Mitigation Using Active Power Filter: A Technologial Review," VOL. 8, NO. 2, pp.17-26 ELEKTRIKA, Malaysia, 2006.
[27] D. –H. Chen and S. –J. Xie, "Review of Control Strategies Applied to Active Power Filters," Proceedings of the IEEE International Conference on Electric Utility Deregulation, Restructuring and Power Technologies (DRPT), Hong Kong, pp. 666-670, 2004.

XI. BIOGRAPHIES

Mohamed Amin Moftah was born in Asyut in 1975. He had his B.Sc. and M.Sc. degrees in Electrical Engineering from Asyut University, Egypt. He worked as electrical preparation and instrumentation engineer in Asyut Cement Company from 1998-2000 then he moved to Egyptian Electricity Transmission Company (EETC) as HV/EHV substation protection and testing engineer. He had been appointed from 2011-2013 as an electrical technical Instructor for power system protection & control in Saudi Electricity Company (SEC), Dammam Training Center, KSA. Then he worked from 2014-2016 as projects design Coordinator for western operation area (WOA) NGrid SEC Jeddah KSA. He participated in upgrading electrical network of Middle Egypt Electricity zone, EETC, Asyut Networks section as a design reviewer officer engineer for new projects and extension of existing S/Ss. His current research areas include power quality issues, power system analysis, renewable energy applications and DG resources.

El-Nobi Ahmed Ibrahim was born in Luxor, Egypt in 1960. He received his B.Sc., M.Sc. and Ph.D. from Asyut University, Egypt in 1984 and 1990, and 1996 respectively, all in Electrical Engineering. He is currently an assistant Member Professor at the Department of Electrical Engineering, Asyut University, Egypt. His main research interests are planning, application of artificial intelligent techniques on power systems, control systems, optimization, analysis, simulation and design of electrical systems.

Gaber El-Saady Ahmed Taha born in Aswan, Egypt in 1959. He received his B.Sc., M.Sc. and Ph.D. from Asyut University, Egypt in 1982 and 1988, and 1995 respectively, all in Electrical Engineering. He was Demonstrator from 1982–1988, he worked as a teaching assistant till 1995. He was a staff member as Associate Professor from 2000, he has been a professor since 2006 at Electrical Engineering Department, Asyut University. He supervised the "Center for Maintenance and Repair of Scientific Appliances" in Asyut University from 2010-2014. His fields of interest include power system analysis, DG systems, modeling, fuzzy logic controller, innovative systems design, phase induction motor, simulated annealing algorithm, applied simulation, and power electronics control applied to renewable energy and power quality systems such as active power filters, PWM rectifiers.